ACS APPLIED MATERIALS & INTERFACES

Research Article

www.acsami.org

Compact Bis-Adduct Fullerenes and Additive-Assisted Morphological Optimization for Efficient Organic Photovoltaics

Yun-Yu Lai, Ming-Hung Liao, Yen-Ting Chen, Fong-Yi Cao, Chain-Shu Hsu, and Yen-Ju Cheng*

Department of Applied Chemistry, National Chiao Tung University, 1001 University Road, Hsin-Chu, 30010 Taiwan

Supporting Information

ABSTRACT: Bis-adduct fullerenes surrounded by two insulating addends sterically attenuate intermolecular interaction and cause inferior electron transportation. In this research, we have designed and synthesized a new class of bis-adduct fullerene materials, methylphenylmethano-C_{60} bis-adduct ($MPC_{60}BA$), methylthienylmethano-C_{60} bis-adduct ($MTC_{60}BA$), methylphenylmethano-C_{70} bis-adduct ($MPC_{70}BA$), and methylthienylmethano-C_{70} bis-adduct ($MTC_{70}BA$), functionalized with two compact phenylmethylmethano and thienylmethylmethano addends via cyclopropyl linkages. These materials with much higher-lying lowest unoccupied molecular orbital (LUMO) energy levels successfully enhanced the V_{oc} values of the P3HT-based solar cell devices. The compact phenylmethylmethano and thienylmethylmethano addends to promote fullerene intermolecular interactions result in aggregation-induced phase separation as observed by the atomic force microscopy (AFM) and transmission electron microscopy (TEM) images of the poly(3-hexylthiophene-2,5-diyl) (P3HT)/bis-adduct fullerene thin films. The device based on the P3HT/$MTC_{60}BA$ blend yielded a V_{oc} of 0.72 V, a J_{sc} of 5.87 mA/cm^2, and a fill factor (FF) of 65.3%, resulting in a power conversion efficiency (PCE) of 2.76%. The unfavorable morphologies can be optimized by introducing a solvent additive to fine-tune the intermolecular interactions. 1-Chloronaphthalene (CN) having better ability to dissolve the bis-adduct fullerenes can homogeneously disperse the fullerene materials into the P3HT matrix. Consequently, the aggregated fullerene domains can be alleviated to reach a favorable morphology. With the assistance of CN additive, the P3HT/$MTC_{60}BA$-based device exhibited enhanced characteristics (a V_{oc} of 0.78 V, a J_{sc} of 9.04 mA/cm^2, and an FF of 69.8%), yielding a much higher PCE of 4.92%. More importantly, the additive-assisted morphological optimization is consistently effective to all four compact bis-adduct fullerenes regardless of the methylphenylmethano or methylthienylmethano scaffolds as well as C_{60} or C_{70} core structures. Through the extrinsic additive treatment, these bis-adduct fullerene materials with compact architectures show promise for high-performance polymer solar cells.

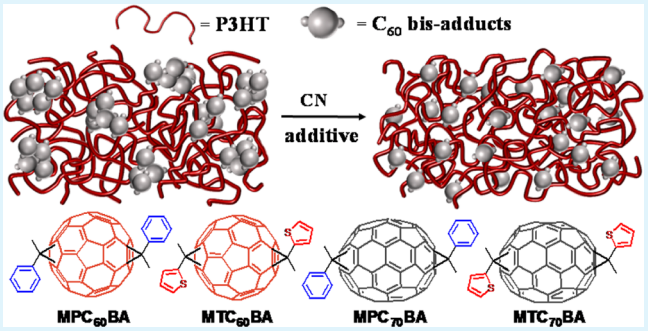

KEYWORDS: *bis-adduct fullerenes, polymers, additive, morphology, aggregation, solar cells*

INTRODUCTION

Bulk heterojunction (BHJ) solar cells containing a mixture of photoactive donor and acceptor materials have attracted enormous academic and industrial attention.[1−6] Fullerene derivatives have been the most widely used n-type materials in BHJ photovoltaics due to their low-lying lowest unoccupied molecular orbital (LUMO) energy levels, fast photoinduced electron transfer, and high electron mobilities.[7−12] The power conversion efficiency (PCE) of photovoltaic devices is governed by open-circuit voltage (V_{oc}), short-circuit current density (J_{sc}), and fill factor (FF). It is known that the magnitude of V_{oc} is generally proportional to the energy offset between the highest occupied molecular orbital (HOMO) energy level of the donor and the LUMO level of the acceptor.[13−15] Therefore, raising the LUMO energy level of a fullerene acceptor is regarded as a practical way to obtain a greater V_{oc} value. Compared to a monoadduct fullerene, saturating two double bonds in a C_{60} or C_{70} results in the formation of a bis-adduct fullerene with a notable upward shift of the LUMO energy level.[9,16−45] However, the implantation of two insulating addends on a fullerene might sterically shield the spherical surface from close packing. The higher content of insulting moieties as well as the attenuation of intermolecular interaction of a bis-adduct fullerene would reduce its electron mobility and decrease the photocurrent of the device, resulting in a trade-off between V_{oc} and J_{sc}.[46] Therefore, using a more compact addend to construct a bis-adduct fullerene could be a solution to maintain higher-lying LUMO energy levels without sacrificing charge transport capability. The well-known monoadduct phenyl-C_{61}-butyric acid methyl ester (PCBM) and bis-adduct PCBM use (butyric acid methyl ester)phenyl methano moiety as the addends through cyclopropyl groups as the linkage. By cutting of the butyric acid methyl ester moiety in

Received: August 23, 2014
Accepted: October 6, 2014
Published: October 6, 2014

the bis-adduct PCBM, herein we design and synthesize a methylphenylmethano C_{60} bis-adduct ($MPC_{60}BA$) and a methylphenylmethano C_{70} bis-adduct ($MPC_{70}BA$) using a more compact phenylmethylmethano addend. Besides, their thiophene-based analogues, methylthienylmethano C_{60} bis-adduct ($MTC_{60}BA$) and methylthienylmethao C_{70} bis-adduct ($MTC_{70}BA$), were also designed and synthesized, respectively (Scheme 1). The $MPC_{60}BA$, $MPC_{70}BA$, $MTC_{60}BA$, and $MTC_{70}BA$ materials functionalized with two compact addends via cyclopropanation are expected to enhance intermolecular interactions between the fullerene cages for facile charge transportation. Nevertheless, these compact fullerene architectures could also give rise to aggregation-induced phase separation, which turns out to reduce the p/n interfacial area. Incorporation of a solvent additive into a binary blending system has been commonly used to manipulate the donor/acceptor interactions and alter the morphology. This strategy is particularly effective and successful for various low band gap conjugated polymers[47−65] and small molecules[66,67] in combination with $PC_{61}BM$ or $PC_{71}BM$. Despite the fact that some bis-adduct fullerene materials have been developed, utilizing the additive strategy to optimize the morphology of the bis-adduct fullerene-based binary systems is only sporadically reported and worthy of in-depth investigation.[68] In this research, morphological engineering using an additive strategy will be employed to tailor the morphology of P3HT/bis-adduct fullerenes. We found that 1-chloronaphthalene (CN) is able to intercalate the bis-adduct fullerenes into the P3HT polymer network to suppress them from severe aggregation. With the assistance of CN additive, more homogeneous P3HT/bis-adduct fullerenes blends with nanoscaled phase separation and bicontinuous network were obtained. The morphological optimization benefits the exciton dissociation and charge transportation. By employing the structural modification and the solvent additive strategy, the P3HT/$MTC_{60}BA$-based device yielded the highest PCE of 4.92% with a V_{oc} of 0.78 V.

Scheme 1. Chemical Structures of $PC_{61}BM$, Bis-$PC_{61}BM$, $MPC_{60}BA$, $MTC_{60}BA$, $MPC_{70}BA$, and $MTC_{70}BA$

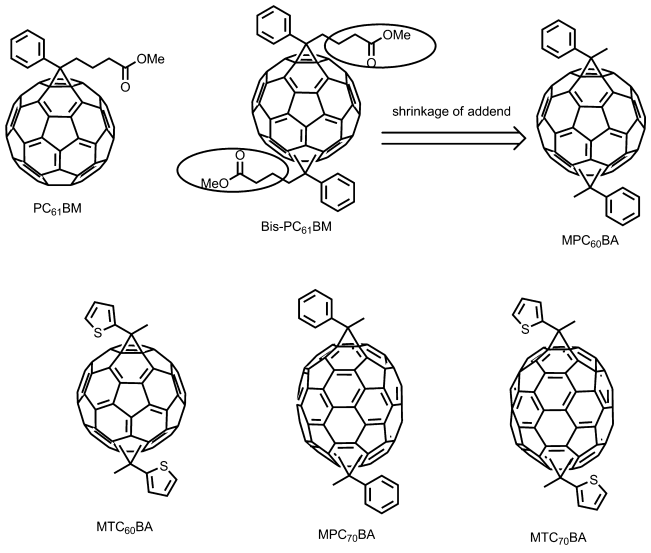

RESULTS AND DISCUSSION

Synthesis. The synthetic routes for the bis-adduct fullerene materials are shown in Scheme 2. The acetophenone (**1a**) and 2-acetylthiophene (**1b**) were first converted to the corresponding tosylhydrazone compounds **2a** and **2b**. In the presence of NaH, two equivalents of compound **2** were reacted with C_{60} or C_{70} to furnish the corresponding $MPC_{60}BA$, $MTC_{60}BA$, $MPC_{70}BA$, and $MTC_{70}BA$ bis-adducts, respectively. These bis-adduct isomers were separated from the monoadduct and tris-adduct isomers by multiple chromatography. ^{1}H NMR spectra of the materials indicated that the final products are a mixture of regioisomers.

Thermal Properties. Thermogravimetric analysis (TGA) and differential scanning calorimetry (DSC) were used to investigate the thermal properties (Figures 1 and 2). The bis-adduct fullerenes exhibited notably high decomposition temperatures (T_d) at 5% weight loss (613 °C for $MPC_{60}BA$, 535 °C for $MPC_{70}BA$, 513 °C for $MTC_{60}BA$, and 447 °C for $MTC_{70}BA$). The methylphenylmethano scaffolds on fullerenes resulted in higher thermal stability than the methylthienylmethano scaffolds. It should be noted that the well-known indene-C_{60} bis-adduct (ICBA) fullerene exhibited much lower T_d of 250 °C because of the retro Diels−Alder reaction.[69] This result reveals that the cyclopropyl moiety is a superb bis-adduct linkage in terms of thermal stability.

Compared to $PC_{61}BM$, the bis-adduct fullerenes showed relatively broad endothermic melting transitions above 250 °C in the DSC measurements, suggesting that a mixture of

Scheme 2. Synthetic Routes of $MPC_{60}BA$, $MTC_{60}BA$, $MPC_{70}BA$, and $MTC_{70}BA$

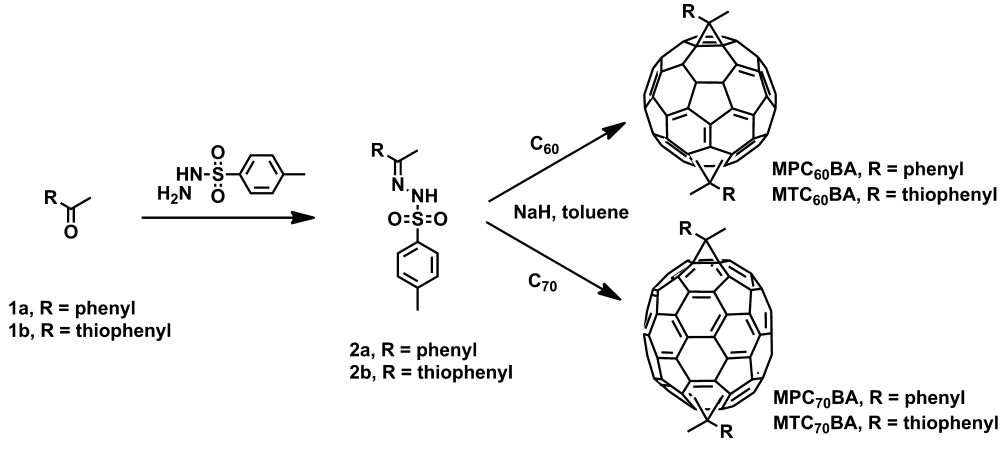

dx.doi.org/10.1021/am505616x | ACS Appl. Mater. Interfaces 2014, 6, 20102−20109

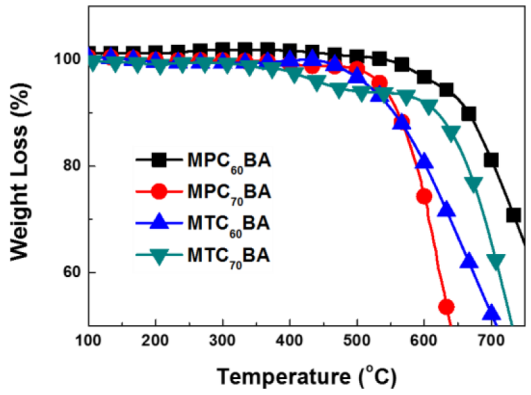

Figure 1. Thermogravimetric analysis (TGA) measurement of the bis-adduct fullerenes with a heating rate of 10 °C/min.

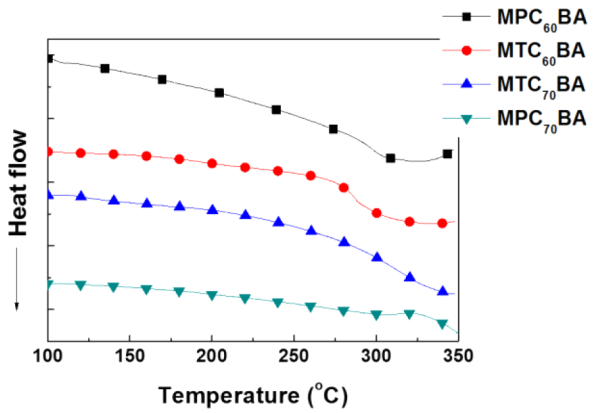

Figure 2. Differential scanning calorimetry (DSC) measurement of the bis-adduct fullerenes with a heating rate of 10 °C/min.

regioisomers leads to more irregular molecular packing (Figure 2).

Optical Properties. UV–vis spectra of the bis-adduct fullerenes and $PC_{61}BM$ in the toluene were measured under the concentration of 10^{-5} M for comparison (as shown in Figure 3). $MTC_{60}BA$ and $MPC_{60}BA$ showed stronger absorption intensity than $PC_{61}BM$. $MTC_{70}BA$ and $MPC_{70}BA$ indeed exhibited stronger and broader absorption compared to their

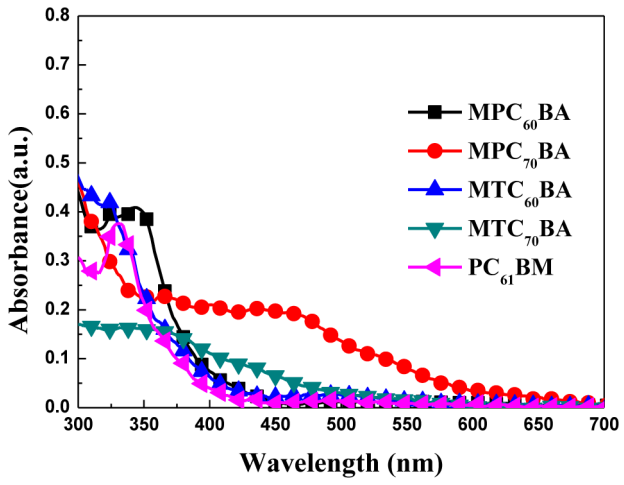

Figure 3. Absorption spectra of the bis-adduct fullerenes in toluene solutions (10^{-5} mol/L).

C_{60} analogues in the visible region of 400–700 nm.[70] These results indicate that the bis-adduct fullerenes offer an advantage over $PC_{61}BM$ on light-harvesting capability.

Electrochemical Properties. The electrochemical properties of these materials were investigated by cyclic voltammetry in Figure 4. There are three well-defined and reversible redox waves

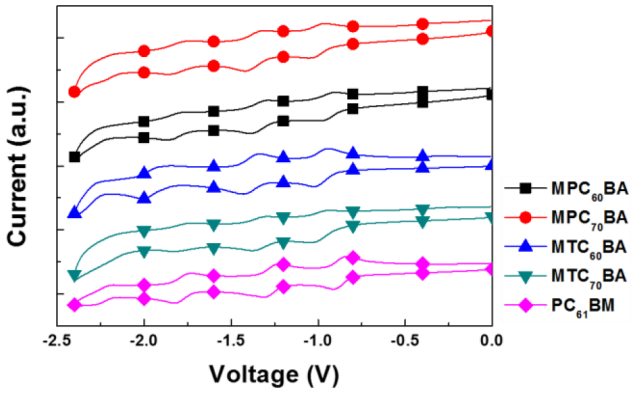

Figure 4. Cyclic voltammetry of the bis-adduct fullerenes at a scan rate of 100 mV/s.

for the four materials in the potential ranging from 0 to −2.5 V. The first reduction potential of these materials shifts negatively by ca. 0.1 eV compared to that of $PC_{61}BM$. The LUMO energy levels of the four materials are estimated to be ca. −3.80 eV regardless of methylthienylmethano or methylphenylmethano scaffold on C_{60} or C_{70}. Because of the much higher-lying LUMO energy levels, enhanced V_{oc} values of the P3HT/bis-adduct-based devices could be expected. The onset values of the first reduction potentials and the estimated LUMO energy levels of the bis-adduct fullerene derivatives are listed in Table 1.

Table 1. Onset Values of the First Reduction Potentials and the Estimated LUMO Energy Levels of the Bis-Adduct Fullerenes

	$MTC_{60}BA$	$MTC_{70}BA$	$MPC_{60}BA$	$MPC_{70}BA$	$PC_{61}BM$
first reduction potential (V)	−0.89	−0.88	−0.87	−0.90	−0.8
LUMO (eV)	−3.81	−3.82	−3.83	−3.80	−3.90

Photovoltaic and Electron-Mobility Characteristics. To evaluate these bis-adduct fullerene materials, the BHJ solar cells based on the configuration of (indium tin oxide (ITO)/poly(3,4-ethylenedioxythiophene) polystyrene sulfonate (PEDOT:PSS)/P3HT:bis-adduct fullerene/Ca/Al) were fabricated and characterized under simulated 100 mW/cm^2 AM 1.5 G illumination. The current density–voltage curves of the devices are shown in Figure 5; the corresponding device characteristics with the optimal blending ratio are shown in Table 2.

All the devices using the bis-adduct fullerenes showed the much improved V_{oc} values compared to that of traditional P3HT/$PC_{61}BM$-based devices. However, the devices exhibited inferior current densities, which could be presumably ascribed to the severe aggregation of the bis-adduct fullerenes, resulting in reduction of p/n junction interfaces and depression of exciton dissociation. The device using P3HT/$MTC_{60}BA$ blend (1:1 wt %) exhibits a V_{oc} of 0.72 V, a J_{sc} of 5.87 mA/cm^2, and an FF of 65.3%, resulting in a PCE of 2.76%. The unfavorable morphology can be optimized by introducing a small amount 1-chloronaph-

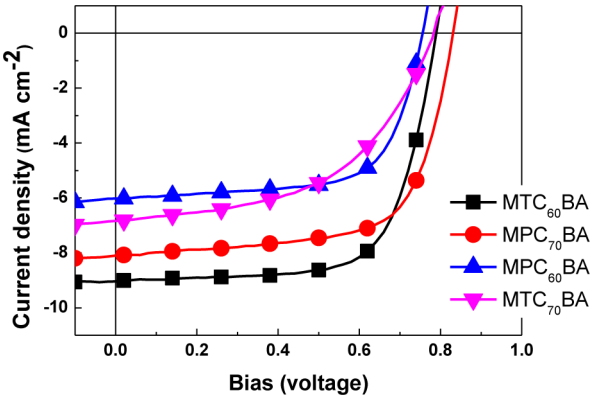

Figure 5. Current density−voltage characteristics of ITO/PEDOT:PSS/P3HT:bis-adduct fullerene/Ca/Al devices under illumination of AM 1.5 G with 100 mW/cm^2.

Table 2. Device Characteristics Based on (ITO/PEDOT:PSS/P3HT:Bis-Adduct Fullerene/Ca/Al) Configuration

P3HT:bis-adduct fullerene	V_{oc} (V)	J_{sc} (mA/cm^2)	FF (%)	PCE (%)
$MPC_{60}BA$ (1:0.6 in wt %) without CN	0.76	5.53	60.1	2.55
$MPC_{60}BA$ (1:0.6 in wt %) with 5 wt % CN	0.76	6.02	66.7	3.05
$MTC_{60}BA$ (1:1 in wt %) without CN	0.72	5.87	65.3	2.76
$MTC_{60}BA$ (1:1 in wt %) with 3 wt % CN	0.78	9.04	69.8	4.92
$MPC_{70}BA$ (1:1 in wt %) without CN	0.78	6.04	60.4	2.84
$MPC_{70}BA$ (1:1 in wt %) with 5 wt % CN	0.86	8.02	67.0	4.50
$MTC_{70}BA$ (1:0.6 in wt %) without CN	0.78	7.05	58.2	3.20
$MTC_{70}BA$ (1:0.6 in wt %) with 5 wt % CN	0.80	7.27	66.1	3.84
$PC_{61}BM$ (1:1 in wt %)	0.62	9.75	58.3	3.52

thalene (CN) as the processing additive in the active layer. The P3HT/$MTC_{60}BA$ blend (1:1 wt %)-based device with 3 wt % CN showed significant improvement of performance with a V_{oc} of 0.78 V, a J_{sc} of 9.04 mA/cm^2, an FF of 69.8%, and a PCE of 4.92%. Similarly, the device based on P3HT/$MPC_{70}BA$ blend (1:1 wt %) originally delivered a V_{oc} of 0.78 V, a J_{sc} of 6.04 mA/cm^2, an FF of 60.4%, and a PCE of 2.84%, but showed a dramatically improved PCE of 4.5% when 5 wt % CN was introduced (a V_{oc} of 0.86 V, a J_{sc} of 8.0 mA/cm^2, and an FF of 67%). The positive effect of the CN additive is also applicable to the $MTC_{70}BA$ and $MPC_{60}BA$ systems. After incorporating 5 wt % CN additive, the P3HT/$MTC_{70}BA$-based device improved the PCE from 3.2% to 3.84%, while the device using P3HT/$MPC_{60}BA$ improved the PCE from 2.55% to 3.05%. The new class of bis-adduct fullerene materials exhibit higher FF but lower J_{sc} compared with the reference $PC_{61}BM$. Bis-adduct fullerenes contain a mixture of isomers that may sterically and electronically affect the electron transportation.[34]

Morphological Optimization. The surface morphology of the P3HT/bis-adduct fullerene blends were investigated by atomic force microscopy (AFM) shown in Figure 6. The images of P3HT/$MTC_{60}BA$ (1:1 in wt %), P3HT/$MPC_{60}BA$ (1:0.6 in wt %), P3HT/$MTC_{70}BA$ (1:0.6 in wt %), and P3HT/$MPC_{70}BA$ (1:1 in wt %) thin films prepared by spin-coating showed obvious phase separation due to the strong aggregation of the bis-adduct fullerenes. This implies that these bis-adduct fullerenes with compact addends have stronger intermolecular interactions. In sharp contrast, the domain size in the AFM phase images became much smaller when the CN additive was introduced, indicating that the fullerene aggregation is significantly alleviated. The phenomena were consistently observed in all four P3HT/bis-adduct fullerene materials, indicating that using CN additive is a general approach to improve the morphology of these compact bis-adduct fullerenes. These results are in good agreement with the improved current densities and fill factors of the devices. Transmission electron microscopy (TEM) was also used to observe the morphological evolution before and after adding CN (Figure 7). Without using CN, the microsized cracks were observed in the P3HT/$MTC_{60}BA$ film as a result of severe phase separation of the active layer. Nevertheless, these cracks disappeared in the film in the presence of 3 wt % CN. These results are consistent with the morphological evolution of the AFM images.

The hole and electron mobilities in the binary blends were evaluated by the space-charge limited current (SCLC) method. The electron-only devices (ITO/ZnO/P3HT:bis-adduct fullerene/Ca/Al) and the hole-only devices (ITO/PEDOT:PSS/P3HT:bis-adduct fullerene/Au) were fabricated (Table 3). The active layer morphologies in the hole- and electron-only devices have been optimized by using the CN additive conditions described above. The bis-adduct fullerenes generally exhibited slower electron mobilities than $PC_{61}BM$. Nevertheless, the $MPC_{60}BA$-, $MTC_{60}BA$-, $MPC_{70}BA$-, and $MTC_{70}BA$-based devices showed comparable or even higher electron mobilities than the $PC_{61}BM$-based device (ca. 10^{-5} cm^2/(V s)) (Table 3). This indicates that the compact fullerene architecture benefits the electron hopping. Furthermore, P3HT/bis-adduct fullerenes showed similar hole mobilities, suggesting the bis-adduct fullerenes do not affect P3HT polymer packing. It is also noteworthy that the thiophene-containing $MTC_{60}BA$ and $MTC_{70}BA$ devices exhibited higher hole mobilities than the phenyl-containing $MPC_{60}BA$ nad $MPC_{70}BA$ devices.

CONCLUSIONS

We have designed a new class of bis-adduct fullerenes $MPC_{60}BA$, $MTC_{60}BA$, $MPC_{70}BA$, and $MTC_{70}BA$ by introducing two compact methylphenylmethano and methylthienylmethano scaffolds on C_{60} and C_{70}, respectively. These materials, synthesized by one-step double cyclopropanation, possess much high-lying LUMO energy levels of ca. −3.8 eV to successfully achieve higher V_{oc} values (0.76−0.86 V) in comparison with the P3HT/$PC_{61}BM$-based device (0.62 V). The P3HT/bis-adduct fullerene thin films exhibited severe phase separation due to the strong intermolecular interactions between the compact spherical structures of the fullerene materials. The fullerene aggregation leads to a significant reduction in p/n interfaces, which are responsible for much lower short-circuit currents of the P3HT/bis-adduct fullerene devices. For instance, the device using P3HT/$MTC_{60}BA$ showed a decent V_{oc} of 0.72 V and FF of 65% but a poor J_{sc} of 5.87 mA/cm^2 and, thus, a limited PCE of 2.76%. To circumvent this morphological problem, we found that 1-chloronaphthalene (CN) is an effective additive to prevent severe aggregation. By incorporating 5 wt % CN as an additive, the device exhibited an improved V_{oc} of 0.78 V, a J_{sc} of 9.04 mA/cm^2, and a fill factor of 69.8%, leading to a higher PCE of 4.92%. Similarly, the PCE of the P3HT/$MPC_{70}BA$-based device improved from 2.84% to 4.5% after using 5 wt % CN additive. The P3HT/$MTC_{70}BA$-based devices (from 3.20% to

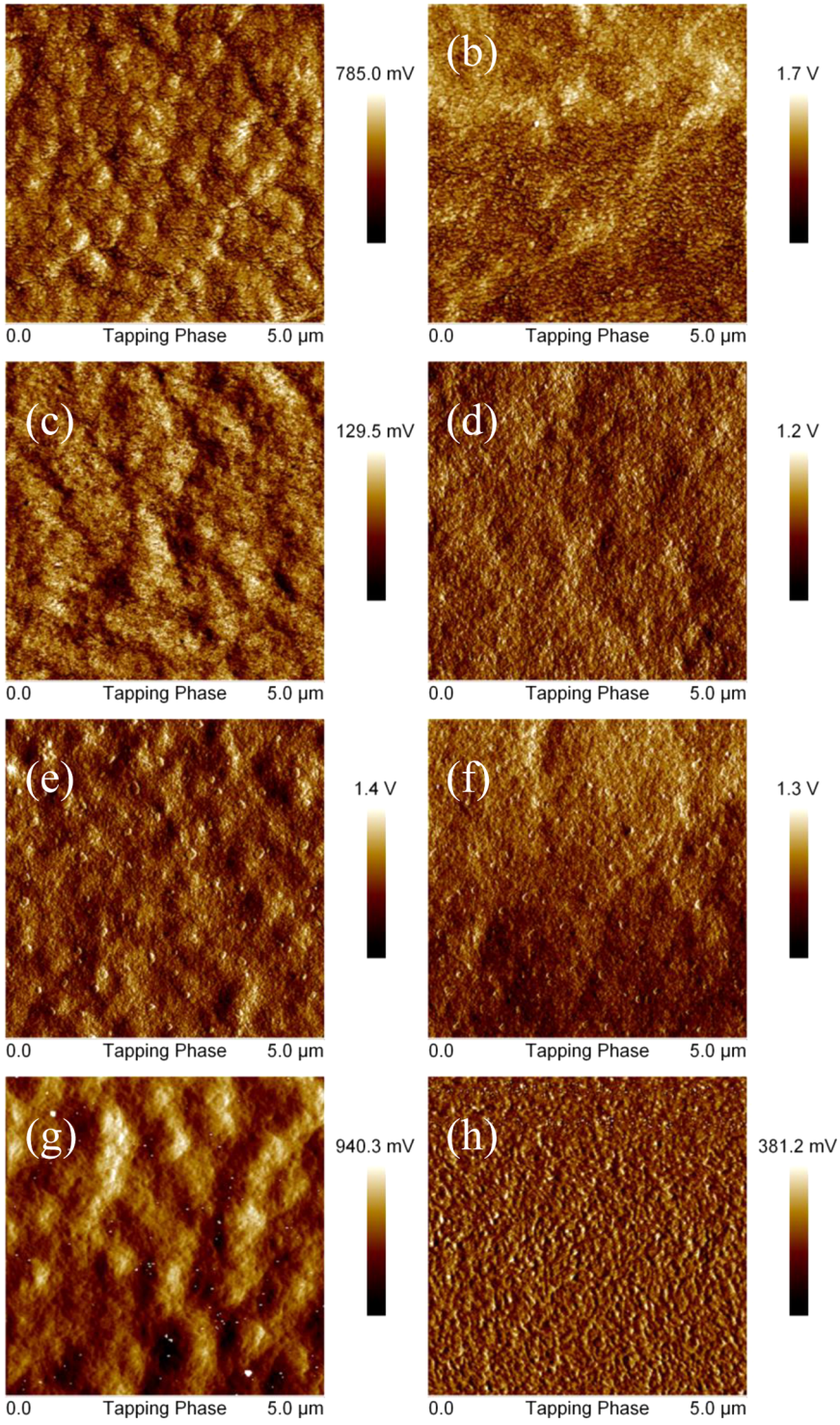

Figure 6. Atomic force microscopy phase images of the blends before adding CN (a) P3HT/MTC$_{60}$BA (1:1 in wt %), (c) P3HT/MPC$_{60}$BA (1:0.6 in wt %), (e) P3HT/MTC$_{70}$BA (1:0.6 in wt %), and (g) P3HT/MPC$_{70}$BA (1:1 in wt %) blends; after adding CN (b) P3HT/MTC$_{60}$BAwith 3 wt % CN, (d) P3HT/MPC$_{60}$BA with 5 wt % CN, (f) P3HT/MTC$_{70}$BA with 5 wt % CN, and (h) P3HT/MPC$_{70}$BA with 5 wt % CN.

3.84%) and P3HT/MPC$_{60}$BA-based devices (from 2.55% to 3.05%) also showed improved performance. With the assistance of CN additive to well disperse fullerene materials into the P3HT matrix, the more homogeneous P3HT/bis-adduct fullerenes thin films were formed. Therefore, the electron mobilities and J_{sc} values were significantly improved. By combining intrinsic structural modification and extrinsic additive treatment to control the intermolecular fullerene interactions, the compact bis-adduct fullerene materials with high synthetic efficacy are promising for high-performance polymer solar cells.

EXPERIMENTAL SECTION

Synthesis of Compound MTC$_{60}$BA. To a toluene solution (1 L) of compound **2b** (0.66 g, 2.24 mmol) was added sodium hydride (0.26 g, 10.8 mmol) quickly under nitrogen. After the solution was stirred at room temperature for 20 min, C$_{60}$ (0.8 g, 1.11 mmol) was added. The

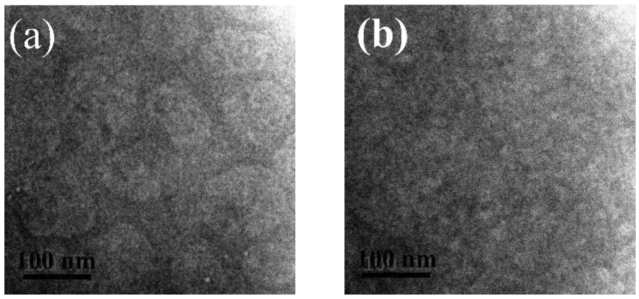

Figure 7. Transmission electron microscopy (TEM) images of P3HT/$MTC_{60}BA$ (1:1 wt %) (a) before adding CN and (b) after adding 3 wt % CN.

Table 3. Carrier Mobilities of the Blends Extracted from the Space-Charge Limited Current Method

P3HT:bis-adduct fullerenes with CN	hole mobility[a] ($cm^2/V\,s$)	electron mobility[b] ($cm^2/V\,s$)
$MPC_{60}BA$ (1:0.6 wt %)	1.4×10^{-4}	2.3×10^{-5}
$MTC_{60}BA$ (1:1 wt %)	2.8×10^{-4}	1.8×10^{-5}
$MPC_{70}BA$ (1:1 wt %)	5.6×10^{-5}	3.2×10^{-5}
$MTC_{70}BA$ (1:0.6 wt %)	1.5×10^{-4}	5.6×10^{-5}
$PC_{61}BM$ (1:1 wt %)	9.4×10^{-5}	2.1×10^{-5}

[a]Hole-only devices based on (ITO/PEDOT:PSS/P3HT:bis-adduct fullerene/Au). [b]Electron-only devices based on (ITO/ZnO/P3HT:bis-adduct fullerene/Ca/Al).

solution was heated to reflux at 120 °C for 24 h. After cooling to room temperature, the solution was extracted with $NH_4Cl_{(aq)}$. The organic layer was dried over anhydrous $MgSO_4$, and the solvent was removed by concentration. Finally, the mixture was loaded into a silica gel column, using toluene and hexane (v/v, 1/4) as the eluent. The solid was reprecipitated in methanol from toluene five times. The brown solid was filtered and washed twice with methanol and dried overnight under vacuum to get the red−brown $MTC_{60}BA$ (85 mg, 8%). MS (FAB) m/z: 940.

Synthesis of Compound $MTC_{70}BA$. In a similar manner described above, $MTC_{70}BA$ was obtained from **2b** (95 mg, 13%). MS (FAB) m/z: 1060.

Synthesis of Compound $MPC_{60}BA$. In a similar manner described above, $MPC_{60}BA$ was obtained from **2a** (100 mg, 15%). MS (FAB) m/z: 928.

Synthesis of Compound $MPC_{70}BA$. In a similar manner described above, $MPC_{70}BA$ was obtained from **2a** (80 mg, 10%). MS (FAB) m/z: 1048.

General Measurement and Characterization. All chemicals were purchased from Aldrich and Acros, unless otherwise specified. ^1H spectra were recorded on a Varian Unity-300 spectrometer. Differential scanning calorimetry (DSC) was measured on TA Q200 Instrument under a nitrogen atmosphere at a heating rate of 10 °C/min, and thermogravimetric analysis (TGA) was recorded on a PerkinElmer Pyris system under nitrogen atmosphere at a heating rate of 20 °C/min. Absorption spectra were collected on a Hitachi U-4100 spectrophotometer. Electrochemical cyclic voltammetry (CV) was conducted on a CH Instruments electrochemical analyzer as the workstation. A carbon glass was used as the working electrode, Pt wire was used as the counter electrode, and Ag/Ag^+ electrode (0.01 M $AgNO_3$, 0.1 M tetrabutylammonium perchlorate (TBAP) in acetonitrile) was used as the reference electrode in a mixed solution of *o*-dichlorobenzene/acetonitrile (4:1) with 0.1 M tetrabutylammonium hexafluorophosphate ($TBAPF_6$) at 100 mV/s. LUMO = −e ($E_{red\ on}$ + 4.75), where $E_{red\ on}$ is the onset reduction potential (in volts) versus Ag/Ag^+. The AFM images under tapping mode were taken on a Veeco INNOVA Microscope AFM system with a INNOVA Nanodrive controller.

Transmission Electron Microscopy (TEM) Observation. TEM observations were performed in bright-field, high-resolution mode on a JEOL JEM-2010 transmission electron microscope with an accelerating voltage of 200 kV equipped with a Gatan-831 charge-coupled device (CCD) camera. The thin-film sample was first spin-coated onto a ITO substrate covered with 40 nm of PEDOT:PSS. The sample was then immersed into water to dissolve the PEDOT:PSS layer and separate the thin films from the ITO substrate. Thin films floated on a water surface were picked up by copper grids coated with an amorphous carbon layer, dried under vacuum overnight, and used in the TEM observations.

Device Fabrication and Characterization. The ITO/glass substrates were first cleaned in ultrasonic baths of isopropyl alcohol, acetone, and isopropyl alcohol, respectively. These were treated with UV−ozone for 20 min. Then, the surface of the ITO substrate was modified by spin-coating PEDOT:PSS solution (Clevios P AI4083), followed by baking at 170 °C for 15 min in a glovebox. The mixture solution of P3HT (18 mg) and bis-adduct fullerenes (18 mg) ($MTC_{60}BA$, $MPC_{70}BA$) or P3HT (13 mg) and bis-adduct fullerenes (7.8 mg) ($MPC_{60}BA$, $MTC_{70}BA$) in 1 mL of *o*-dichlorobenzene (ODCB) was then spin-coated onto the PEDOT:PSS layer. The P3HT:bis-adduct fullerene blend film was then put into glass Petri dishes while still wet, to undergo a solvent annealing process. After drying, the samples were annealed at 150 °C for 10 min prior to the cathode electrode deposition. The cathode, which was made of calcium (35 nm thick) and aluminum (100 nm thick), was sequentially evaporated through a shadow mask under high vacuum ($<10^{-6}$ Torr). Each sample consists of four independent pixels defined by an active area of 0.04 cm^2. Finally, the devices were encapsulated and characterized in air. The devices were characterized under 100 mW/cm^2 AM 1.5 simulated light measurement (Yamashita Denso solar simulator). Current density ($J-V$) characteristics of devices were obtained by a Keithley Model 2400 SMU system. Solar illumination conforming the JIS Class AAA was provided by a SAN-EI 300W solar simulator equipped with an AM 1.5G filter. The light intensity was calibrated with a Hamamatsu S1336-5BK silicon photodiode. The performances presented here are the average of the four pixels of each device. To investigate the electron mobilities of the different blend films, unipolar devices have been prepared following the same procedure except that the PEDOT:PSS layer is replaced by evaporated ZnO (40 nm). For the hole-only device, Al is replaced by evaporated Au (40 nm). The electron and hole mobilities were calculated according to space-charge limited current (SCLC) theory. The $J-V$ curves were fitted according to the following equation: $J = (9/8)\varepsilon\mu(V^2/L^3)$ where ε is the permittivity of the blend film, μ is the hole mobility, and L is the film thickness.

■ ASSOCIATED CONTENT

Supporting Information

Solid-state absorption spectra, ^1H NMR spectra, and mass spectrometry of the materials. This material is available free of charge via the Internet at http://pubs.acs.org.

■ AUTHOR INFORMATION

Corresponding Author

*E-mail: yjcheng@mail.nctu.edu.tw.

Notes

The authors declare no competing financial interest.

■ ACKNOWLEDGMENTS

We thank the Ministry of Science and Technology and the Ministry of Education, and Center for Interdisciplinary Science (CIS) of the National Chiao Tung University, Taiwan, for financial support. Y.-J.C. gives thanks for the support from the Golden-Jade fellowship of the Kenda Foundation and the Foundation of the Advancement of Outstanding Scholarship (FAOS) in Taiwan.

REFERENCES

(1) Arias, A. C.; MacKenzie, J. D.; McCulloch, I.; Rivnay, J.; Salleo, A. Materials and Applications for Large Area Electronics: Solution-Based Approaches. *Chem. Rev.* **2010**, *110*, 3−24.

(2) Günes, S.; Neugebauer, H.; Sariciftci, N. S. Conjugated Polymer-Based Organic Solar Cells. *Chem. Rev.* **2007**, *107*, 1324−1338.

(3) Li, Y. Molecular Design of Photovoltaic Materials for Polymer Solar Cells: Toward Suitable Electronic Energy Levels and Broad Absorption. *Acc. Chem. Res.* **2012**, *45*, 723−733.

(4) Coakley, K. M.; McGehee, M. D. Conjugated Polymer Photovoltaic Cells. *Chem. Mater.* **2004**, *16*, 4533−4542.

(5) Zhan, X.; Zhu, D. Conjugated Polymers for High-Efficiency Organic Photovoltaics. *Polym. Chem.* **2010**, *1*, 409−419.

(6) Cheng, Y.-J.; Yang, S.-H.; Hsu, C.-S. Synthesis of Conjugated Polymers for Organic Solar Cell Applications. *Chem. Rev.* **2009**, *109*, 5868−5923.

(7) Thompson, B. C.; Fréchet, J. M. J. Polymer−Fullerene Composite Solar Cells. *Angew. Chem., Int. Ed.* **2008**, *47*, 58−77.

(8) He, Y.; Li, Y. Fullerene Derivative Acceptors for High Performance Polymer Solar Cells. *Phys. Chem. Chem. Phys.* **2011**, *13*, 1970−1983.

(9) Li, C.-Z.; Yip, H.-L.; Jen, A. K. Y. Functional Fullerenes for Organic Photovoltaics. *J. Mater. Chem.* **2012**, *22*, 4161−4177.

(10) Lai, Y.-Y.; Cheng, Y.-J.; Hsu, C.-S. Applications of Functional Fullerene Materials in Polymer Solar Cells. *Energy Environ. Sci.* **2014**, *7*, 1866−1883.

(11) Anthony, J. E.; Facchetti, A.; Heeney, M.; Marder, S. R.; Zhan, X. n-Type Organic Semiconductors in Organic Electronics. *Adv. Mater.* **2010**, *22*, 3876−3892.

(12) Chen, H.-Y.; Hou, J.; Zhang, S.; Liang, Y.; Yang, G.; Yang, Y.; Yu, L.; Wu, Y.; Li, G. Polymer Solar Cells with Enhanced Open-Circuit Voltage and Efficiency. *Nat. Photonics* **2009**, *3*, 649−653.

(13) Brabec, C. J.; Cravino, A.; Meissner, D.; Sariciftci, N. S.; Fromherz, T.; Rispens, M. T.; Sanchez, L.; Hummelen, J. C. Origin of the Open Circuit Voltage of Plastic Solar Cells. *Adv. Funct. Mater.* **2001**, *11*, 374−380.

(14) Scharber, M. C.; Mühlbacher, D.; Koppe, M.; Denk, P.; Waldauf, C.; Heeger, A. J.; Brabec, C. J. Design Rules for Donors in Bulk-Heterojunction Solar Cells—Towards 10% Energy-Conversion Efficiency. *Adv. Mater.* **2006**, *18*, 789−794.

(15) Koster, L. J. A.; Mihailetchi, V. D.; Blom, P. W. M. Ultimate Efficiency of Polymer/Fullerene Bulk Heterojunction Solar Cells. *Appl. Phys. Lett.* **2006**, *88*, 093511.

(16) Lenes, M.; Wetzelaer, G.-J. A. H.; Kooistra, F. B.; Veenstra, S. C.; Hummelen, J. C.; Blom, P. W. M. Fullerene Bisadducts for Enhanced Open-Circuit Voltages and Efficiencies in Polymer Solar Cells. *Adv. Mater.* **2008**, *20*, 2116−2119.

(17) He, Y.; Chen, H.-Y.; Hou, J.; Li, Y. Indene−C_{60} Bisadduct: A New Acceptor for High-Performance Polymer Solar Cells. *J. Am. Chem. Soc.* **2010**, *132*, 1377−1382.

(18) Hsieh, C.-H.; Cheng, Y.-J.; Li, P.-J.; Chen, C.-H.; Dubosc, M.; Liang, R.-M.; Hsu, C.-S. Highly Efficient and Stable Inverted Polymer Solar Cells Integrated with a Cross-Linked Fullerene Material as an Interlayer. *J. Am. Chem. Soc.* **2010**, *132*, 4887−4893.

(19) Cheng, Y.-J.; Hsieh, C.-H.; He, Y.; Hsu, C.-S.; Li, Y. Combination of Indene-C_{60} Bis-Adduct and Cross-Linked Fullerene Interlayer Leading to Highly Efficient Inverted Polymer Solar Cells. *J. Am. Chem. Soc.* **2010**, *132*, 17381−17383.

(20) Zhao, G.; He, Y.; Li, Y. 6.5% Efficiency of Polymer Solar Cells Based on Poly(3-hexylthiophene) and Indene-C_{60} Bisadduct by Device Optimization. *Adv. Mater.* **2010**, *22*, 4355−4358.

(21) Ye, G.; Chen, S.; Xiao, Z.; Zuo, Q.; Wei, Q.; Ding, L. *o*-Quinodimethane-methano[60]Fullerene and Thieno-*o*-quinodimethane-methano[60]Fullerene as Efficient Acceptor Materials for Polymer Solar Cells. *J. Mater. Chem.* **2012**, *22*, 22374−22377.

(22) Han, G. D.; Collins, W. R.; Andrew, T. L.; Bulović, V.; Swager, T. M. Cyclobutadiene−C_{60} Adducts: N-Type Materials for Organic Photovoltaic Cells with High V_{OC}. *Adv. Funct. Mater.* **2013**, *23*, 3061−3069.

(23) Liu, C.; Xu, L.; Chi, D.; Li, Y.; Liu, H.; Wang, J. Synthesis of Novel Acceptor Molecules of Mono- and Multiadduct Fullerene Derivatives for Improving Photovoltaic Performance. *ACS Appl. Mater. Interfaces* **2012**, *5*, 1061−1069.

(24) Kim, K.-H.; Kang, H.; Nam, S. Y.; Jung, J.; Kim, P. S.; Cho, C.-H.; Lee, C.; Yoon, S. C.; Kim, B. J. Facile Synthesis of *o*-Xylenyl Fullerene Multiadducts for High Open Circuit Voltage and Efficient Polymer Solar Cells. *Chem. Mater.* **2011**, *23*, 5090−5095.

(25) Zhang, C.; Chen, S.; Xiao, Z.; Zuo, Q.; Ding, L. Synthesis of Mono- and Bisadducts of Thieno-*o*-quinodimethane with C_{60} for Efficient Polymer Solar Cells. *Org. Lett.* **2012**, *14*, 1508−1511.

(26) Cheng, Y.-J.; Liao, M.-H.; Chang, C.-Y.; Kao, W.-S.; Wu, C.-E.; Hsu, C.-S. Di(4-methylphenyl)methano-C_{60} Bis-Adduct for Efficient and Stable Organic Photovoltaics with Enhanced Open-Circuit Voltage. *Chem. Mater.* **2011**, *23*, 4056−4062.

(27) Li, C.-Z.; Chien, S.-C.; Yip, H.-L.; Chueh, C.-C.; Chen, F.-C.; Matsuo, Y.; Nakamura, E.; Jen, A. K. Y. Facile Synthesis of a 56π-Electron 1,2-Dihydromethano-[60]PCBM and its Application for Thermally Stable Polymer Solar Cells. *Chem. Commun.* **2011**, *47*, 10082−10084.

(28) He, Y.; Peng, B.; Zhao, G.; Zou, Y.; Li, Y. Indene Addition of [6,6]-Phenyl-C_{61}-butyric Acid Methyl Ester for High-Performance Acceptor in Polymer Solar Cells. *J. Phys. Chem. C* **2011**, *115*, 4340−4344.

(29) Meng, X.; Zhang, W.; Tan, Z. a.; Li, Y.; Ma, Y.; Wang, T.; Jiang, L.; Shu, C.; Wang, C. Highly Efficient and Thermally Stable Polymer Solar Cells with Dihydronaphthyl-Based [70]Fullerene Bisadduct Derivative as the Acceptor. *Adv. Funct. Mater.* **2012**, *22*, 2187−2193.

(30) Kim, K.-H.; Kang, H.; Kim, H. J.; Kim, P. S.; Yoon, S. C.; Kim, B. J. Effects of Solubilizing Group Modification in Fullerene Bis-Adducts on Normal and Inverted Type Polymer Solar Cells. *Chem. Mater.* **2012**, *24*, 2373−2381.

(31) Li, Y. Fullerene-Bisadduct Acceptors for Polymer Solar Cells. *Chem.—Asian J.* **2013**, *8*, 2316−2328.

(32) He, Y.; Zhao, G.; Peng, B.; Li, Y. High-Yield Synthesis and Electrochemical and Photovoltaic Properties of Indene-C_{70} Bisadduct. *Adv. Funct. Mater.* **2010**, *20*, 3383−3389.

(33) Meng, X.; Zhao, G.; Xu, Q.; Tan, Z. a.; Zhang, Z.; Jiang, L.; Shu, C.; Wang, C.; Li, Y. Effects of Fullerene Bisadduct Regioisomers on Photovoltaic Performance. *Adv. Funct. Mater.* **2014**, *24*, 158−163.

(34) Liao, M.-H.; Lai, Y.-Y.; Lai, Y.-Y.; Chen, Y.-T.; Tsai, C.-E.; Liang, W.-W.; Cheng, Y.-J. Reducing Regioisomers of Fullerene-Bisadducts by Tether-Directed Remote Functionalization: Investigation of Electronically and Sterically Isomeric Effects on Bulk-Heterojunction Solar Cells. *ACS Appl. Mater. Interfaces* **2013**, *6*, 996−1004.

(35) Guo, X.; Zhang, M.; Cui, C.; Hou, J.; Li, Y. Efficient Polymer Solar Cells Based on Poly(3-hexylthiophene) and Indene−C_{60} Bisadduct Fabricated with Non-halogenated Solvents. *ACS Appl. Mater. Interfaces* **2014**, *6*, 8190−8198.

(36) Cheng, P.; Li, Y.; Zhan, X. Efficient Ternary Blend Polymer Solar Cells with Indene-C_{60} Bisadduct as an Electron-Cascade Acceptor. *Energy Environ. Sci.* **2014**, *7*, 2005−2011.

(37) Ye, L.; Zhang, S.; Qian, D.; Wang, Q.; Hou, J. Application of Bis-PCBM in Polymer Solar Cells with Improved Voltage. *J. Phys. Chem. C* **2013**, *117*, 25360−25366.

(38) Yang, T.; Jiang, Z.; Huang, X.; Wei, H.; Yuan, J.; Yue, W.; Li, Y.; Ma, W. Design and Synthesis of Soluble Dibenzosuberane-Substituted Fullerene Derivatives for Bulk-Heterojunction Polymer Solar Cells. *Org. Electron.* **2013**, *14*, 2184−2191.

(39) Umeyama, T.; Imahori, H. Design and Control of Organic Semiconductors and Their Nanostructures for Polymer−Fullerene-Based Photovoltaic Devices. *J. Mater. Chem. A* **2014**, *2*, 11545−11560.

(40) Chen, S.; Ye, G.; Xiao, Z.; Ding, L. Efficient and Thermally Stable Polymer Solar Cells Based on a 54π-Electron Fullerene Acceptor. *J. Mater. Chem. A* **2013**, *1*, 5562−5566.

(41) He, D.; Zuo, C.; Chen, S.; Xiao, Z.; Ding, L. A Highly Efficient Fullerene Acceptor for Polymer Solar Cells. *Phys. Chem. Chem. Phys.* **2014**, *16*, 7205−7208.

(42) He, D.; Du, X.; Xiao, Z.; Ding, L. Methanofullerenes, $C_{60}(CH_2)_n$ (n = 1, 2, 3), as Building Blocks for High-Performance Acceptors Used in Organic Solar Cells. *Org. Lett.* **2014**, *16*, 612−615.
(43) Chen, S.; Xiao, Z.; He, D.; Ma, L.; Ding, L. Function of CH_2 Addends on 54π Fullerene Acceptors. *Asian J. Org. Chem.* **2014**, *3*, 936−939.
(44) Kang, H.; Cho, C.-H.; Cho, H.-H.; Kang, T. E.; Kim, H. J.; Kim, K.-H.; Yoon, S. C.; Kim, B. J. Controlling Number of Indene Solubilizing Groups in Multiadduct Fullerenes for Tuning Optoelectronic Properties and Open-Circuit Voltage in Organic Solar Cells. *ACS Appl. Mater. Interfaces* **2012**, *4*, 110−116.
(45) Xiao, Z.; He, D.; Zuo, C.; Gan, L.; Ding, L. An Azafullerene Acceptor for Organic Solar Cells. *RSC Adv.* **2014**, *4*, 24029−24031.
(46) MacKenzie, R. C. I.; Frost, J. M.; Nelson, J. A Numerical Study of Mobility in Thin Films of Fullerene Derivatives. *J. Chem. Phys.* **2010**, *132*, 064904.
(47) Peet, J.; Kim, J. Y.; Coates, N. E.; Ma, W. L.; Moses, D.; Heeger, A. J.; Bazan, G. C. Efficiency Enhancement in Low-Bandgap Polymer Solar Cells by Processing with Alkane Dithiols. *Nat. Mater.* **2007**, *6*, 497−500.
(48) Lee, J. K.; Ma, W. L.; Brabec, C. J.; Yuen, J.; Moon, J. S.; Kim, J. Y.; Lee, K.; Bazan, G. C.; Heeger, A. J. Processing Additives for Improved Efficiency from Bulk Heterojunction Solar Cells. *J. Am. Chem. Soc.* **2008**, *130*, 3619−3623.
(49) Moulé, A. J.; Meerholz, K. Controlling Morphology in Polymer−Fullerene Mixtures. *Adv. Mater.* **2008**, *20*, 240−245.
(50) Moulé, A. J.; Meerholz, K. Morphology Control in Solution-Processed Bulk-Heterojunction Solar Cell Mixtures. *Adv. Funct. Mater.* **2009**, *19*, 3028−3036.
(51) Woo, C. H.; Beaujuge, P. M.; Holcombe, T. W.; Lee, O. P.; Fréchet, J. M. J. Incorporation of Furan into Low Band-Gap Polymers for Efficient Solar Cells. *J. Am. Chem. Soc.* **2010**, *132*, 15547−15549.
(52) Lou, S. J.; Szarko, J. M.; Xu, T.; Yu, L.; Marks, T. J.; Chen, L. X. Effects of Additives on the Morphology of Solution Phase Aggregates Formed by Active Layer Components of High-Efficiency Organic Solar Cells. *J. Am. Chem. Soc.* **2011**, *133*, 20661−20663.
(53) Rogers, J. T.; Schmidt, K.; Toney, M. F.; Kramer, E. J.; Bazan, G. C. Structural Order in Bulk Heterojunction Films Prepared with Solvent Additives. *Adv. Mater.* **2011**, *23*, 2284−2288.
(54) Su, M.-S.; Kuo, C.-Y.; Yuan, M.-C.; Jeng, U. S.; Su, C.-J.; Wei, K.-H. Improving Device Efficiency of Polymer/Fullerene Bulk Heterojunction Solar Cells Through Enhanced Crystallinity and Reduced Grain Boundaries Induced by Solvent Additives. *Adv. Mater.* **2011**, *23*, 3315−3319.
(55) Dang, M. T.; Wuest, J. D. Using Volatile Additives to Alter the Morphology and Performance of Active Layers in Thin-Film Molecular Photovoltaic Devices Incorporating Bulk Heterojunctions. *Chem. Soc. Rev.* **2013**, *42*, 9105−9126.
(56) Hu, X.; Wang, M.; Huang, F.; Gong, X.; Cao, Y. 23% Enhanced Efficiency of Polymer Solar Cells Processed with 1-Chloronaphthalene as the Solvent Additive. *Synth. Met.* **2013**, *164*, 1−5.
(57) Bartelt, J. A.; Douglas, J. D.; Mateker, W. R.; Labban, A. E.; Tassone, C. J.; Toney, M. F.; Fréchet, J. M. J.; Beaujuge, P. M.; McGehee, M. D. Controlling Solution-Phase Polymer Aggregation with Molecular Weight and Solvent Additives to Optimize Polymer-Fullerene Bulk Heterojunction Solar Cells. *Adv. Energy Mater.* **2014**, *4*, 10.1002/aenm.201301733.
(58) Schmidt, K.; Tassone, C. J.; Niskala, J. R.; Yiu, A. T.; Lee, O. P.; Weiss, T. M.; Wang, C.; Fréchet, J. M. J.; Beaujuge, P. M.; Toney, M. F. A Mechanistic Understanding of Processing Additive-Induced Efficiency Enhancement in Bulk Heterojunction Organic Solar Cells. *Adv. Mater.* **2014**, *26*, 300−305.
(59) Hoven, C. V.; Dang, X.-D.; Coffin, R. C.; Peet, J.; Nguyen, T.-Q.; Bazan, G. C. Improved Performance of Polymer Bulk Heterojunction Solar Cells Through the Reduction of Phase Separation via Solvent Additives. *Adv. Mater.* **2010**, *22*, E63−E66.
(60) Fan, H.; Zhang, M.; Guo, X.; Li, Y.; Zhan, X. Evolved Phase Separation toward Balanced Charge Transport and High Efficiency in Polymer Solar Cells. *ACS Appl. Mater. Interfaces* **2011**, *3*, 3646−3653.
(61) Karak, S.; Homnick, P. J.; Della Pelle, A. M.; Bae, Y.; Duzhko, V. V.; Liu, F.; Russell, T. P.; Lahti, P. M.; Thayumanavan, S. Crystallinity and Morphology Effects on a Solvent-Processed Solar Cell Using a Triarylamine-Substituted Squaraine. *ACS Appl. Mater. Interfaces* **2014**, *6*, 11376−11384.
(62) Synooka, O.; Kretschmer, F.; Hager, M. D.; Himmerlich, M.; Krischok, S.; Gehrig, D.; Laquai, F.; Schubert, U. S.; Gobsch, G.; Hoppe, H. Modification of the Active Layer/PEDOT:PSS Interface by Solvent Additives Resulting in Improvement of the Performance of Organic Solar Cells. *ACS Appl. Mater. Interfaces* **2014**, *6*, 11068−11081.
(63) Wang, D. H.; Kyaw, A. K. K.; Pouliot, J.-R.; Leclerc, M.; Heeger, A. J. Enhanced Power Conversion Efficiency of Low Band-Gap Polymer Solar Cells by Insertion of Optimized Binary Processing Additives. *Adv. Energy Mater.* **2014**, *4*, 10.1002/aenm.201300835.
(64) Gong, X.; Liu, C.; Hu, X.; Zhong, C.; Huang, M.; Wang, K.; Zhang, Z.; Cao, Y.; Heeger, A. Influence of Binary Processing Additives on the Performance of Polymer Solar Cells. *Nanoscale* **2014**, DOI: 10.1039/C4NR04958F.
(65) Venkatesan, S.; Adhikari, N.; Chen, J.; Ngo, E. C.; Dubey, A.; Galipeau, D. W.; Qiao, Q. Interplay of Nanoscale Domain Purity and Size on Charge Transport and Recombination Dynamics in Polymer Solar Cells. *Nanoscale* **2014**, *6*, 1011−1019.
(66) Sun, Y.; Welch, G. C.; Leong, W. L.; Takacs, C. J.; Bazan, G. C.; Heeger, A. J. Solution-Processed Small-Molecule Solar Cells with 6.7% Efficiency. *Nat. Mater.* **2012**, *11*, 44−48.
(67) Kyaw, A. K. K.; Wang, D. H.; Luo, C.; Cao, Y.; Nguyen, T.-Q.; Bazan, G. C.; Heeger, A. J. Effects of Solvent Additives on Morphology, Charge Generation, Transport, and Recombination in Solution-Processed Small-Molecule Solar Cells. *Adv. Energy Mater.* **2014**, *4*, 10.1002/aenm.201301469.
(68) Guo, X.; Cui, C.; Zhang, M.; Huo, L.; Huang, Y.; Hou, J.; Li, Y. High Efficiency Polymer Solar Cells Based on Poly(3-hexylthiophene)/Indene-C_{70} Bisadduct with Solvent Additive. *Energy Environ. Sci.* **2012**, *5*, 7943−7949.
(69) Wong, W. W. H.; Subbiah, J.; White, J. M.; Seyler, H.; Zhang, B.; Jones, D. J.; Holmes, A. B. Single Isomer of Indene-C_{70} Bisadduct—Isolation and Performance in Bulk Heterojunction Solar Cells. *Chem. Mater.* **2014**, *26*, 1686−1689.
(70) Wienk, M. M.; Kroon, J. M.; Verhees, W. J. H.; Knol, J.; Hummelen, J. C.; van Hal, P. A.; Janssen, R. A. J. Efficient Methano[70]fullerene/MDMO-PPV Bulk Heterojunction Photovoltaic Cells. *Angew. Chem., Int. Ed.* **2003**, *42*, 3371−3375.